

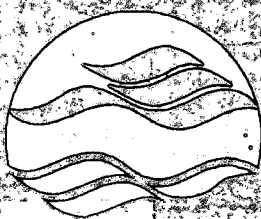
97-101



Environment  
Canada

Environnement  
Canada

Canada



NATIONAL WATER  
RESEARCH INSTITUTE

INSTITUT NATIONAL DE  
RECHERCHE SUR LES EAUX

TD  
226  
N87  
No. 97-  
101

# A Method For Measuring The Transport Properties of a Formation Using a Single Well

BY:

K. Novakowski, P. Lapcevic, J. Voralek

NWRI Contribution No. 97-101

17-101

# **A METHOD FOR MEASURING THE TRANSPORT PROPERTIES OF A FORMATION USING A SINGLE WELL**

BY  
K.S. NOVAKOWSKI,  
P.A. LAPCEVIC,  
J.A. VORALEK,

NATIONAL WATER RESEARCH INSTITUTE  
867 LAKESHORE ROAD  
BURLINGTON, ONTARIO  
L7R 4A6  
416-336-4610  
e-mail: Kent.Novakowski@CCIW.ca

AND  
E.A. SUDICKY

DEPT. OF EARTH SCIENCES  
UNIVERSITY OF WATERLOO  
WATERLOO, ONT  
N2L 3G1

For submission to:  
WATER RESOURCES RESEARCH  
NWRI Cont. # 97-101  
March, 1997

## **MANAGEMENT PERSPECTIVE**

**Title:** A METHOD FOR MEASURING THE TRANSPORT PROPERTIES OF A FORMATION USING A SINGLE WELL.

**Author(s):** K. Novakowski, P. Lapcevic, J. Voralek, and E. Sudicky

**NWRI Publ. #:**

**Citation:** Submitted to Water Resources Research

**EC Priority/Issue:** To determine the most optimal method for the clean-up of contaminated sites in fractured bedrock or clay environments, a detailed conceptual model must be developed. To develop the conceptual model, characterization of the transport properties of the formation is required. This method is designed to accommodate characterisation at sites where contamination is severe and costs of well drilling are prohibitive. This is a deliverable under the Environment Canada Action Plan issue Toxics and addresses the ESD Business Plan Result Thrust 3 (Action on other toxics and substances of concern).

The method also has particular relevance to the Smithville contaminated site, which is the most costly, and difficult site on the Canadian side of the Great Lakes Basin. Thus, this method also supports COA Stream 1 initiatives in the area of groundwater and contaminated sites.

**Current Status:** The method is developed and tested and can now be used at Smithville and other contaminated sites.

**Next Steps:** Study is complete. Additional tool for our site investigation tool box.

## ABSTRACT

For some subsurface investigations of contaminant transport, particularly those conducted in consolidated material, the costs related to well construction prohibit the installation of a comprehensive field of monitoring wells. To circumvent this problem, a method for measuring the transport properties of a fractured, low-porosity formation using a single well, was developed. The method involves the injection of fluid and tracer over a short duration, establishing a radial source condition in the formation, following which the natural flow is allowed to carry the tracer back through the injection well where tracer concentration is monitored passively, in situ. To interpret the experimental results, a numerical model was adapted to account for the mass balance of solute in the source/monitoring well during the injection and monitoring periods. In addition, the model accommodates advection-dispersion, adsorption, decay, and matrix diffusion in a framework of fractures having a variety of geometries. To illustrate the use of the method, a field experiment was conducted in a single well intersecting a discrete horizontal fracture in a flat-lying shale and limestone formation. Interpretation of the results agreed well with the interpretation of other tracer experiments conducted previously in the same fracture plane. It was determined through an informal sensitivity analysis that the parameter estimates obtained are robust and unique. This suggests that the method may yield defensible measurements of transport properties such as matrix porosity and groundwater velocity in geological formations that are expensive and difficult to characterize.

## INTRODUCTION

Measuring the transport properties of geological materials is usually conducted at the field scale by monitoring the migration of existing contamination or by conducting a tracer experiment. The most common method for conducting a tracer experiment involves the establishment of an advective flow field into which a tracer is introduced (eg. Gelhar et al., 1992). Subsequent migration of the tracer is monitored in wells located down-gradient from the tracer source and the transport properties estimated by interpretation of the tracer arrival using an analytical or numerical model.

In cases where only one well is available to conduct a tracer experiment, an injection-withdrawal experiment is usually conducted. In this case, groundwater is injected into the well along with a slug or continuous input of tracer. Following a specified period of injection, the flow-field is reversed and the injected water pumped back out. During the pumping phase, the concentration of tracer is monitored in the effluent flow stream. There are two difficulties associated with this method; 1) transient components of the flow field arise during the initiation and cessation of both the injection and pumping periods, and 2) the hydrodynamic dispersion encountered during the forward movement of the tracer is partially reversed during the pumping phase (Heller, 1972). Partial reversal of the hydrodynamic dispersion may obscure other dispersive processes such as matrix diffusion or adsorption.

For fractured-porous media, conditions for conducting tracer experiments are complicated by the influence of significant volumes of water in the source and monitoring wellbores relative to the volume of water present in the fractures nearby. Dilution of tracer during the injection or

withdrawal of fluid imparts an apparent dispersion resulting in overestimates of the hydrodynamic dispersion coefficient (Novakowski, 1992).

To investigate transport phenomena in geological materials, it is also necessary to determine the natural velocity of the migrating groundwater. Because of the difficulties in conducting tracer experiments under conditions of natural gradient (Novakowski et al., 1995), other techniques for determining natural velocity such as the point dilution method (Drost et al., 1968) have been employed. For fractured-porous media where the volume of water retained in the experimental equipment is significantly larger than in the vicinity of the wellbore, point dilution experiments have proven to be lengthy and difficult to conduct (Novakowski et al., 1995). Further, because only the flux of tracer leaving the wellbore is measured, no information on dispersion or matrix diffusion can be obtained.

The purpose of this study is to present a method for determining the transport properties of unconsolidated or fractured-porous media using a tracer experiment conducted in a single well. The method involves injecting fluid and tracer for a specified period of time to establish a source condition in the formation. Subsequent to the end of the injection period, the migration of tracer back through the injection well is allowed to occur under conditions of natural gradient (the drift phase). The concentration of the tracer is monitored passively in the injection well during the drift phase. It is assumed that the transient effect due to injection is small and that little or no reversal of dispersion occurs with this method. To interpret tracer experiments conducted in this fashion, an adaptation to an existing numerical model is conducted. The new model accounts for the

development of the source condition, advection, horizontal and transverse dispersion, transient matrix diffusion, retardation, mixing in the injection well (during both the injection and drift phases), and a non-uniform distribution of fracture aperture. To illustrate the use of the method, the results of a tracer experiment conducted in a discrete well-characterized fracture is interpreted and discussed. A sensitivity analysis is also conducted to estimate the reliability of the interpreted parameters.

## MODEL DEVELOPMENT

To develop the model for the interpretation of injection-drift experiments, separate governing equations and boundary conditions are required for each of the injection and drift phases. To preclude the potential for influence from inertial effects, the mathematical development is undertaken assuming the experiments will be conducted in geological material of low storativity. Thus, steady flow conditions are assumed for both the injection and drift phases. It is further assumed that dispersion in the immediate vicinity of the source well is negligible and a Dirichlet condition can be used to couple the concentration in the source/monitoring well to the concentration in the formation. The mass balance in the source/monitoring well is established for the general case of  $n$  fractures. For an unfractured-porous formation or a double-porosity media with block or spherical geometry,  $n$  is reduced to unity, and matrix porosity set according to the type of medium.

In the following development, only the mass balance equations for the injection and drift phases are presented. To develop the complete model, these equations are coupled to an existing numerical model for solute transport in a double-porosity medium (Sudicky, 1990). Because the existing

numerical model is formulated in the Laplace domain, the coupling process is facilitated by use of the forward Laplace transform on the mass balance equations.

### Injection Phase

During the injection phase, the injection flow field and the introduction of tracer are established simultaneously. Because it is important to establish a symmetrical cross-section of concentration in the formation at the end of the injection phase, only a Dirac source condition in the injection well is accommodated. The material balance for the tracer in the injection well is given by:

$$V_s \frac{dC(t)}{dt} = -C(t) \sum_{i=1}^n \gamma_{Ii} v_i + V_s C_0 \delta(t) - V_s \lambda C(t) \quad [1]$$

where  $V_s$  is the volume of the mixing section in the well,  $C(t)$  is the concentration in the well,  $C_0$  is the initial concentration (spike input),  $\delta$  is the Dirac delta function,  $v_i$  is the velocity in fracture  $i$  at the well face, and  $\lambda$  is the decay constant for the tracer (decay is assumed to occur only in the solution phase). The initial condition for equation [1] is  $C(0)=0$ .

The parameter  $\gamma_{Ii}$  is the cross-sectional area available for flow within the test interval. For horizontally-fractured media,  $\gamma_{Ii} = 2b_i \times 2\pi r_w$  where  $2b_i$  is the aperture of the  $i$ th fracture and  $r_w$  is the well radius. For uniform porosity or double-porosity media,  $\gamma_{Ii} = b \times \theta \times 2\pi r_w$  where  $\theta$  is porosity of the medium through which fluid can pass.

The forward Laplace transform of [1] is:

$$V_s p \bar{C}(p) = -\bar{C}(p) \sum_{i=1}^n \gamma_{Ii} v_i + V_s C_0 - V_s \lambda \bar{C}(p) \quad [2]$$



where  $p$  is the Laplace variable and the overbar indicates the dependent variable which has undergone the transform.

### Drift Phase

At the end of the injection phase a radial distribution of concentration is established in the formation. This becomes the initial condition for the drift phase. For this study, it is assumed that the initial concentration of the solute in the matrix for the drift phase is equal to zero. For injection periods of short duration or in media of low matrix porosity, this assumption likely leads to minimal error.

The material balance for the well during the drift phase is given by:

$$V_s \frac{dC(t)}{dt} = -C(t) \sum_{i=1}^n \gamma_{Di} V_i + \sum_{i=1}^n C_i(x, t) \Big|_{x=0} \gamma_{Di} V_i - V_s \lambda C(t) \quad [3]$$

where  $C_i$  is the concentration entering the well from the formation,  $x=0$  is the arbitrary location of the well in the flow field, and  $\gamma_{Di}$  is  $\frac{1}{2}$  the cross-sectional area of each fracture exposed in the well (or  $\frac{1}{2}$  the entire formation multiplied by porosity) intersecting the borehole multiplied by a correction factor. Because the correction factor is usually 2 for open, uncompleted boreholes (Novakowski et al., 1995), the definition of  $\gamma_{Di}$  is directly equivalent to  $\gamma_{fi}$ .

The initial condition for [3] is determined by the solution for the decay of concentration in the well (equation [1] solved independently), evaluated at the end of the injection phase. Thus, the initial condition is:

$$C(0) = \exp\left\{-\left[\sum_{i=1}^n \frac{\gamma_{Di} V_i}{V_s} + \lambda\right] t_i\right\} C_0 \quad [4]$$

where  $C_0$  is the initial concentration as defined previously for the injection phase, and  $t_i$  is the duration of the injection phase.

The forward Laplace transform of equation [3] is given by:

$$V_s p \bar{C}(p) = -\bar{C}(p) \sum_{i=1}^n V_{di} V_i + \sum_{i=1}^n \bar{C}_i(x, p) \Big|_{x=0} V_{di} V_i - V_s \lambda \bar{C}(p) + V_s C_1 \quad [5]$$

where  $C_1$  is the initial concentration given by equation [4].

### Model Formulation and Verification

To link the mass balance equations with the numerical model of Sudicky (1990), two approaches are followed. For the injection phase, equation [2] was incorporated directly into the code at the point where calculations of the Laplace concentrations are conducted. The same method could not be followed for the drift phase, however, due to the presence of the constant  $C_1$  in equation [5]. Rather, a direct solution of equation [3] was obtained. The solution was derived using the Laplace transform method with analytical inversion. The solution is given by:

$$C(t) = \sum_{i=1}^n \beta_i \int_0^t C_i(\tau) \exp\{-\xi(t-\tau)\} d\tau + C_1 \exp\{-\xi t\} \quad [6]$$

where:

$$\xi = \frac{\sum_{i=1}^n V_{di} V_i}{V_s} \quad \beta_i = \frac{V_{di} V_i}{V_s}$$

and  $\tau$  is a dummy integration variable. Equation [6] was coded outside the numerical model and uses  $C_1$  from the well node in the numerical grid.

To verify the model, the injection phase component was compared to the analytical solution of Novakowski (1992) for radial divergent transport. The comparison was conducted using a numerical grid 60 m in length by 40 m width. The grid was discretised using a triangular mesh having  $\Delta x = \Delta y = 0.33$  m. The conditions were formulated to approximate that for a single fracture of uniform aperture ( $2b = 230 \mu\text{m}$ ) in a formation of low porosity ( $\theta = 1.0\%$ ). A dispersivity,  $\alpha_L$ , in the fracture of 0.10 m was used. A steady flow model, formulated using the finite element method in two dimensions, was used to calculate the velocity field during the injection phase. The velocity calculations are based on a volumetric flow rate of  $6.94 \times 10^{-6} \text{ m}^3/\text{s}$  imposed at a node central to the grid. The velocities used in the semi-analytical model are a function of radial distance (equations [3] and [6] of Novakowski, 1992) and were calculated using the same volumetric flow rate.

Figure 1 shows the results of the numerical transport simulations as compared to the results of the semi-analytical model executed using the same conditions. The data are presented at the nodes of the finite element grid for both the numerical and semi-analytical simulations. The comparison is presented for injection periods of 9 and 40 minutes. Although the numerical model yields concentrations that extend slightly beyond those of semi-analytical model, the agreement between the curves is otherwise very good. The slight discrepancy observed can be attributed to the coarse discretisation used in the numerical model in the vicinity of the source well.

## FIELD EXAMPLE

To illustrate the use of the method and explore the sensitivity of the interpretations, an field experiment was conducted in a discrete fracture which pervades a flat-lying shale and limestone

sequence at a depth of about 10 m. Because the method results in considerable dilution of the initial concentration during the drift phase, a tracer which can be reliably measured over at least four orders of magnitude in concentration is required. Thus, the present experiment was conducted using Lissamine FF, which is known to be conservative in this environment (Novakowski and Lapcevic, 1994), and can be measured using fluorometric methods over 5-6 orders of magnitude in concentration.

### Method and Results

Figure 2 illustrates schematically the equipment used for both the injection and drift phases of the tracer experiment. The equipment configuration was modified from the apparatus used to conduct point dilution experiments (Novakowski et al., 1995). To determine the duration of the injection period and the appropriate volume for the mixing zone, preliminary modeling was conducted using the semi-analytical solution. The intent of the modeling was to determine the optimal conditions for creating a clearly defined source in the fracture, which is symmetrical about the peak concentration (eg. the right-hand curve illustrated in Figure 1). On this basis, a mixing zone of approximately 3.5 L and an optimal duration of injection of 40 minutes at a rate of 0.4 L/min, were determined.

Approximately 0.030 L of 1 g/L solution of tracer was introduced at the initiation of injection followed by clean water for the remainder of the injection period. A total of 16 L of fluid was injected over the 40 minute period. The initial concentration,  $C_0$ , upon arrival of the tracer in the mixing zone was 12.6 mg/L and the final dimensionless concentration,  $C/C_0$ , in the source well at the end of the period of injection was 0.0047. During the course of the injection period, mixing was

conducted advectively by circulating fluid through the mixing zone using a pump located on ground surface. Samples of the circulating fluid were obtained periodically from the circulation tubing. Figure 3 illustrates the decay in concentration in the source borehole plotted semi-logarithmically relative to the initial concentration. Note that relatively uniform mixing conditions were achieved. Assuming a uniform fracture aperture, the source concentration in the fracture should have peaked at approximately  $C/C_0=0.25$  according to the predictive modeling results.

Following the end of the injection period, mixing in the source well continued and the tracer returned from the fracture under natural flow conditions. During this phase, samples were obtained from the well approximately every  $\frac{1}{2}$  hour at first, diminishing to twice daily towards the end of the experiment. The sample volumes were minimized to 5 mL or less so as to prevent disturbance of the flow field in the fracture. The duration of the drift phase was approximately 250 hrs. The peak  $C/C_0$  in the well during this phase was approximately 0.01.

### Interpretation

Interpretation of the experiment was conducted in three stages. During the first stage, the decay of concentration in the source well was simulated using the independent solution to equation [1]. It was found that the fit shown on Figure 3 could only be achieved with a mixing zone volume,  $V_s$ , within the range of 3.0 to 3.3 L, which is slightly less than the calculated volume of 3.5 L. This indicates that not all of the mixing zone volume contributed to the mixing process during injection and underlines the need to obtain accurate samples during the injection phase. The calculated estimate of  $V_s$  was used in the following two stages of interpretation.

During the second stage, the source condition for the drift phase was established using the numerical model. Figure 4 shows the estimated distribution of concentration in any radial direction at the end of the injection and beginning of the drift phase. A new source distribution was used for each attempt at a model fit to the concentration measured during the drift phase.

During the third stage, the numerical model was used to simulate the concentrations obtained during the drift phase. The model fit was achieved using a manual procedure whereby the fracture aperture was uniformly fixed at 242  $\mu\text{m}$  (equal to the aperture determined from a previously-conducted hydraulic test), the volume,  $V_s$ , fixed at 3.5 L, the effective diffusion coefficient for Lissamine fixed at  $1.8 \times 10^{-10} \text{ m}^2/\text{s}$ , and velocity, dispersivity and matrix porosity, varied. The effective diffusion coefficient is based on the free-water diffusion coefficient for Lissamine which is equal to  $4.5 \times 10^{-10} \text{ m}^2/\text{s}$ , multiplied by a geometric factor (Novakowski and van der Kamp, 1996) estimated at 0.4. Because matrix diffusion in the numerical model is formulated by lumping matrix porosity, the geometric factor, and the free-water diffusion coefficient together at the fracture-matrix interface, it is difficult to separate porosity from the geometric factor for the model fits. Thus, it is necessary to use an estimate for this value. This was obtained from the results of a diffusion experiment conducted at the laboratory scale using a similar rock type (Novakowski and van der Kamp, 1996).

Figure 5 shows the experimental results and the model fit. The fit was achieved using a mean groundwater velocity of 5.52 m/day, a dispersivity of 0.10 m, and a matrix porosity of 1.4%. The quality of the fit is very good over all portions of the concentration history. The magnitude of the groundwater velocity estimated using the model agrees well with measurements of velocity obtained

from the results of natural gradient tracer experiments and point dilution experiments conducted in the same portion of the fracture (Novakowski et al., 1995). The values of dispersivity and matrix porosity are also in good agreement with that obtained from the interpretation of a tracer experiment conducted previously over a similar but larger scale (Novakowski and Lapcevic, 1994).

### Sensitivity

To achieve the fit shown in Figure 5, it was found that the location of the peak concentration in time was sensitive to the average groundwater velocity and the magnitude of the peak concentration sensitive to the matrix porosity. During the process of fitting the model to the experimental data, variations in groundwater velocity of  $\pm 0.2$  m/day, variations in dispersivity of  $\pm 0.05$  m, and variations in matrix porosity of  $\pm 0.2\%$  beyond those reported above resulted in fits which were visually unacceptable.

Figure 6 shows the results of example simulations conducted using parameters equal to those used for Figure 5 excepting matrix porosity which was varied over the range of 1-15%. The peak concentration is observed to be quite sensitive to matrix porosity for the conditions used in this field experiment. Note in particular, that the decay in concentration past the peak is strongly dependent on the magnitude of the peak concentration. Thus, the estimate of matrix porosity obtained from the field experiment is likely reliable within the range of visually acceptable fit (ie.  $\pm 0.2\%$ ). However, given the uncertainty related to the geometric factor, a slightly broader range of confidence likely.

Figure 7 shows the influence of dispersivity on the concentration history during the drift phase. This

figure was constructed in the same fashion as Figure 6 with the exception that dispersivity was varied from 0.05 to 1.0 m and matrix porosity was fixed at 1.4 %. In comparison to the influence of matrix porosity as shown in Figure 6, the influence of dispersivity is much less pronounced, particularly in the later-time data. The curves, however, are sensitive to differences in dispersivity at early time, indicating that, similar to the case for matrix porosity, the reliability of the fitting estimate is within the range of visually acceptable fit. In addition, the independence of the late-time data suggests that the model fit shown in Figure 5 is unique.

To further explore the uniqueness of the model fit, a Monte Carlo study using stochastically-generated distributions of fracture aperture, was conducted. The purpose of the study was to investigate the influence of variable aperture in the region of the fracture plane over which the transport processes were measured. Using a mean aperture,  $\langle b \rangle = 242 \mu\text{m}$ , 24 realizations of the aperture distribution were constructed using a direct Fourier transform technique (Robin et al., 1993) for each combination of variance ( $1000 \mu\text{m}^2$  and  $10\,000 \mu\text{m}^2$ ) and correlation length (isotropic at 1.0 m). The numerical model was then run for both the injection and drift phases using each realization. The transport simulations were conducted using the parameters (excluding aperture) obtained from the fit to the experimental data.

Figure 8 shows the ensemble of results for 24 realizations (and the mean of all 24) generated using a variance of  $1000 \mu\text{m}^2$  and a correlation length of 1.0 m and compared to the model fit shown in Figure 5. Thus, for an aperture field having a small variance, the parameters used to fit the experimental data are well estimated. However, at larger variance (Figure 9), there is considerably



more spread in the distribution of possible concentration histories. It is important to note that, because the simulation of the aperture distributions are conducted without conditioning (ie. the aperture at the location of the well node is not fixed to 242  $\mu\text{m}$ ), the well may occur in a region of large or small aperture and thus reflect higher or lower velocity, respectively. However, in the field case, this would be reflected in the aperture determined from the hydraulic test conducted in the well. Thus, the best comparison is made to the average of the 24 Monte Carlo simulations (Figure 9) which shows a very similar curve to that for the constant aperture with the exception of a slight retardation in the arrival time of the peak concentration. On the basis of this similarity, it is suggested that interpretations conducted with uniform aperture will approximate well the parameters related to dispersion and matrix diffusion and slightly over-estimate groundwater velocity

The results of the sensitivity investigation conducted above suggest that this experimental method may provide a very robust and unique means for investigating the transport properties of horizontally fractured media. However, it is important to note that the uniqueness observed in the results and interpretation of the present field experiment, may not be observed in the results of experiments conducted in media where the fracturing is more prodigious. For example, in cases where classical double porosity effects are developed as a result of closely-spaced horizontal and vertical fractures (ie. block geometry), uniqueness may be subverted by uncertainty in the fracture geometry. Further field and modeling investigation are required to explore this.

## CONCLUSIONS

A method to investigate the transport properties of a fractured-porous formation using a single well

is developed and illustrated. The method involves injecting fluid and tracer into the formation for a short period of time, followed by an extended period of monitoring in the injection hole as the tracer drifts back through the well under natural flow conditions. Advective mixing is conducted in the wellbore during both the injection and drift phases. A numerical model was developed by incorporating formal mass balance equations for the wellbore for both the injection and drift phases. The numerical model accounts for solute mixing in the well, advective and dispersive transport in the formation, adsorption, decay, and diffusion from the fractures into the unfractured matrix. The fractures may be horizontal and infinite in lateral extent or form a block geometry. Media of uniform porosity is also accommodated. The numerical model was verified by comparison to a semi-analytical model for the injection phase.

To illustrate the use of the method, a field example was conducted whereby tracer was injected into discrete fracture in a low-porosity shale. The duration of injection was approximately 40 minutes which resulted in a radially-symmetric source condition in the fracture having a maximum penetration of about 6 m. The resulting return of the tracer to the injection well during the drift phase occurred over the following 250 hrs. The peak concentration during the drift phase was only 1% of the concentration at the start of the injection phase. Interpretation of the results using the numerical model provided estimates of dispersivity, velocity, and matrix porosity that agreed well with the results of other experiments conducted in the same fracture. A sensitivity study conducted to investigate the uniqueness of the interpreted parameters showed that each of the velocity, dispersivity, and matrix porosity were sufficiently independent. Thus, unique interpretations were obtained using this method, at least for the conditions encountered in the present field experiment.

In addition, the influence of variable aperture was found not to subvert the uniqueness of the interpretations to a significant degree. Thus, it is suggested that this method may prove to be a powerful tool in the investigation of transport in fractured formations where the cost of drilling limits the number boreholes available to the investigation.

## REFERENCES

Drost, W., D. Klotz, A. Koch, H. Moser, F. Neumaier and W. Rauert, Point dilution methods of investigating groundwater flow by means of radioisotopes, *Water Resour. Res.*, 4(1), 125-146, 1968.

Gelhar, L.W., C. Welty and K.R. Rehfeldt, A critical review of field-scale dispersion in aquifers, *Water Resour. Res.*, 28(7), 1955-1974, 1992.

Heller, J.P., Observations of mixing and diffusion in porous media, in *Proc. Fund. Trans. Phen. Porous Media*, IAHR Symposium, Guelph, Ontario, Aug., 1972.

Novakowski, K.S., P.A. Lapcevic, J. Voralek, and G. Bickerton, Preliminary interpretation of tracer experiments conducted in a discrete rock fracture under conditions of natural flow, *Geophys. Res. Lett.*, 22(11), 1417-1420, 1995.

Novakowski, K.S., and P.A. Lapcevic, Field measurement of radial solute transport in a discrete rock fracture, *Water Resour. Res.*, 30(1), 37-44, 1994.

Novakowski, K.S., and G. van der Kamp, The radial diffusion method. 2. A semi-analytical model for the determination of apparent diffusivity, porosity and adsorption, *Water Resour. Res.*, 32(6), 1823-1830, 1996.

Novakowski, K.S., The analysis of tracer experiments conducted in divergent radial flow fields,

Water Resour. Res., 28(12), 3215-3225, 1992.

Robin, M.J.L., A.L. Gutjahr, E.A. Sudicky and J.L. Wilson, Cross-correlated random field generation with the direct Fourier transform method, Water Resour. Res., 29(7), 2385-2397, 1993.

Sudicky, E.A., The Laplace transform galerkin technique for efficient time-continuous solution of solute transport in double-porosity media, Geoderma, 46, 209-232, 1990.

**LIST OF FIGURES**

- Figure 1. Comparison between the semi-analytical model and numerical model for two injection periods of 9 and 40 minutes duration, respectively.
- Figure 2. Schematic illustration of the apparatus used for the field experiment.
- Figure 3. Decline in concentration in the source well during the injection period. Also shown is the model fit to the experimental data.
- Figure 4. Model simulation of the concentration in the fracture at the end of the injection period and start of the drift phase.
- Figure 5. Concentration history and model fit for the source/monitoring well during the drift phase. Model fit was obtained by visual estimation.
- Figure 6. Influence of matrix porosity on the shape of the concentration history during the drift phase.
- Figure 7. Influence of dispersivity on the shape of the concentration history during the drift phase.
- Figure 8. The results of a Monte Carlo study where transport is simulated in a variable aperture

field having a variance in aperture of  $1000 \mu\text{m}^2$  and an isotropic correlation length of 1.0 m.

**Figure 9.** The results of a Monte Carlo study where transport is simulated in a variable aperture field having a variance in aperture of  $10000 \mu\text{m}^2$  and an isotropic correlation length of 1.0 m.

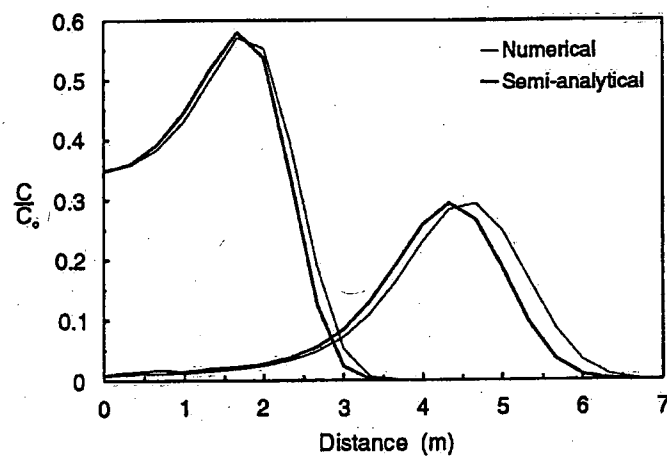


Figure 1. Comparison between the semi-analytical model and numerical model for two injection periods of 9 and 40 minutes duration, respectively.



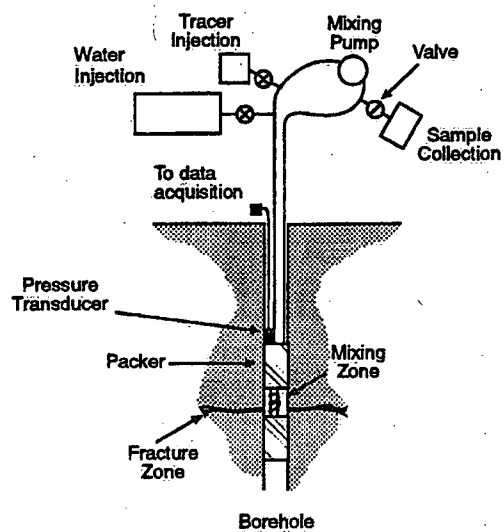


Figure 2. Schematic illustration of the apparatus used for the field experiment.

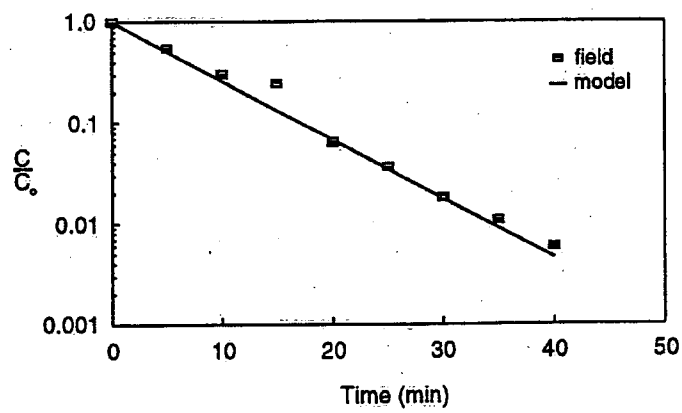


Figure 3. Decline in concentration in the source well during the injection period. Also shown is the model fit to the experimental data.

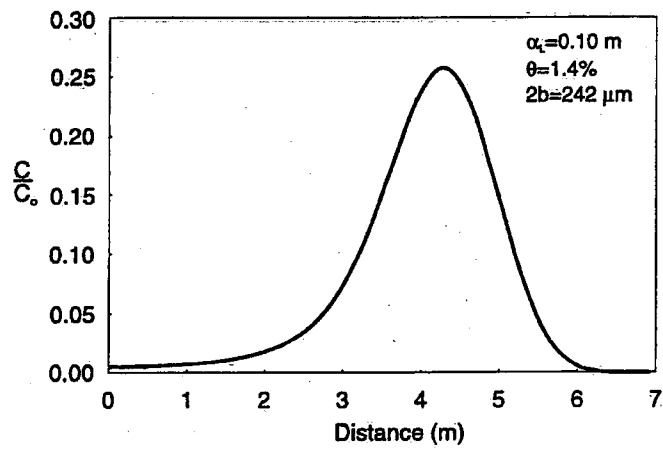


Figure 4. Model simulation of the concentration in the fracture at the end of the injection period and start of the drift phase.

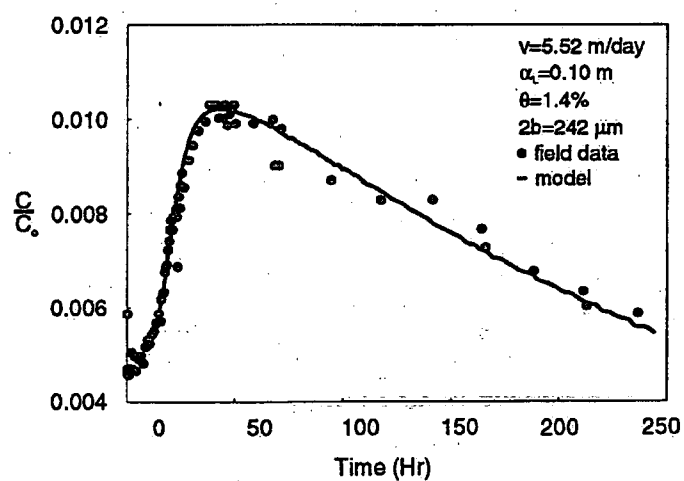


Figure 5. Concentration history and model fit for the source/monitoring well during the drift phase. Model fit was obtained by visual estimation.

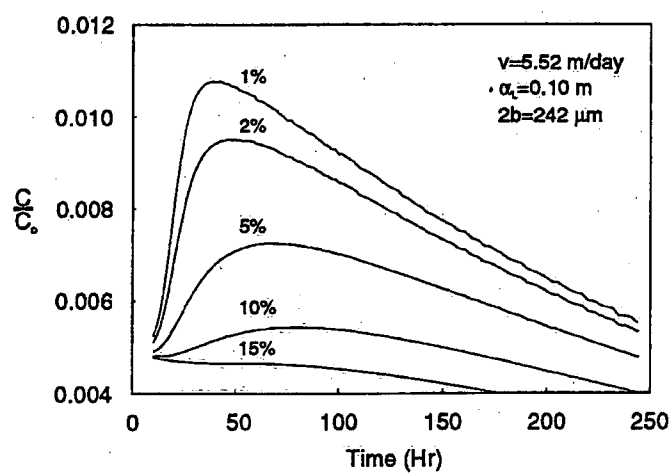


Figure 6. Influence of matrix porosity on the shape of the concentration history during the drift phase.

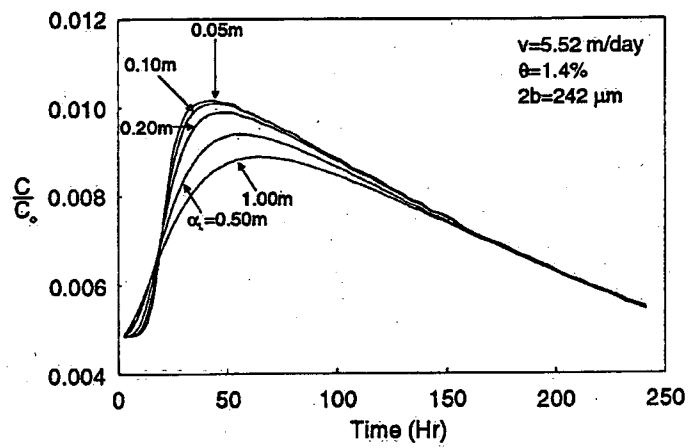


Figure 7. Influence of dispersivity on the shape of the concentration history during the drift phase.

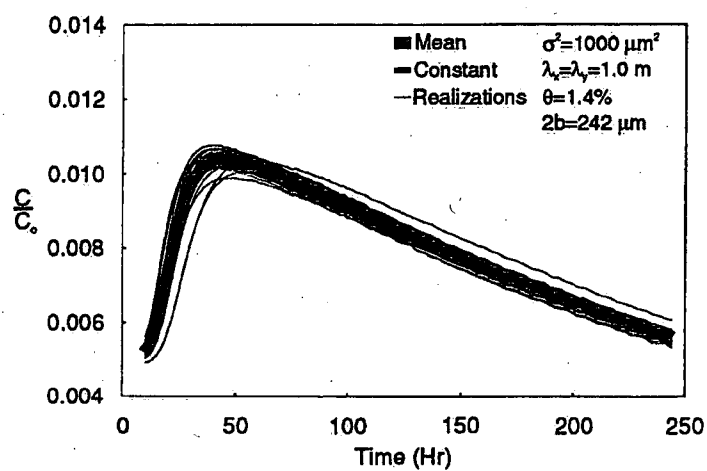


Figure 8. The results of a Monte Carlo study where transport is simulated in a variable aperture field having a variance in aperture of  $1000 \text{ mm}^2$  and an isotropic correlation length of  $1.0 \text{ m}$ .

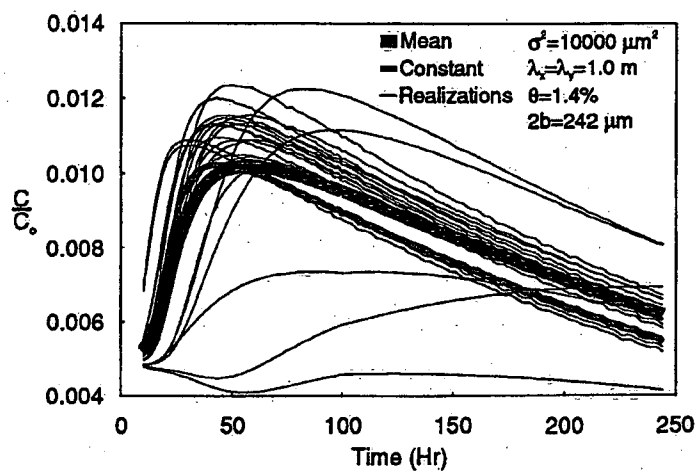


Figure 9. The results of a Monte Carlo study where transport is simulated in a variable aperture field having a variance in aperture of 10000 mm<sup>2</sup> and an isotropic correlation length of 1.0 m.



Environment Canada Library, Burlington



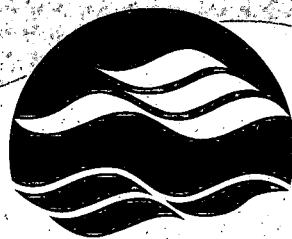
3 9055 1017 8278 6

PRINTED IN CANADA  
IMPRIMERIE AU CANADA



ON RECYCLED PAPER  
SUR DU PAPIER RECYCLÉ

**National Water Research Institute**  
**Environment Canada**  
**Canada Centre for Inland Waters**  
P.O. Box 5050  
867 Lakeshore Road  
Burlington, Ontario  
L7R 4A6 Canada



**NATIONAL WATER  
RESEARCH INSTITUTE**  
**INSTITUT NATIONAL DE  
RECHERCHE SUR LES EAUX**

**National Hydrology Research Centre**  
11 Innovation Boulevard  
Saskatoon, Saskatchewan  
S7N 3H5 Canada

**Institut national de recherche sur les eaux**  
**Environnement Canada**  
**Centre canadien des eaux intérieures**  
Case postale 5050  
867, chemin Lakeshore  
Burlington, Ontario  
L7R 4A6 Canada

**Centre national de recherche en hydrologie**  
11, boul. Innovation  
Saskatoon, Saskatchewan  
S7N 3H5 Canada



Environment  
Canada

Environnement  
Canada

**Canada**